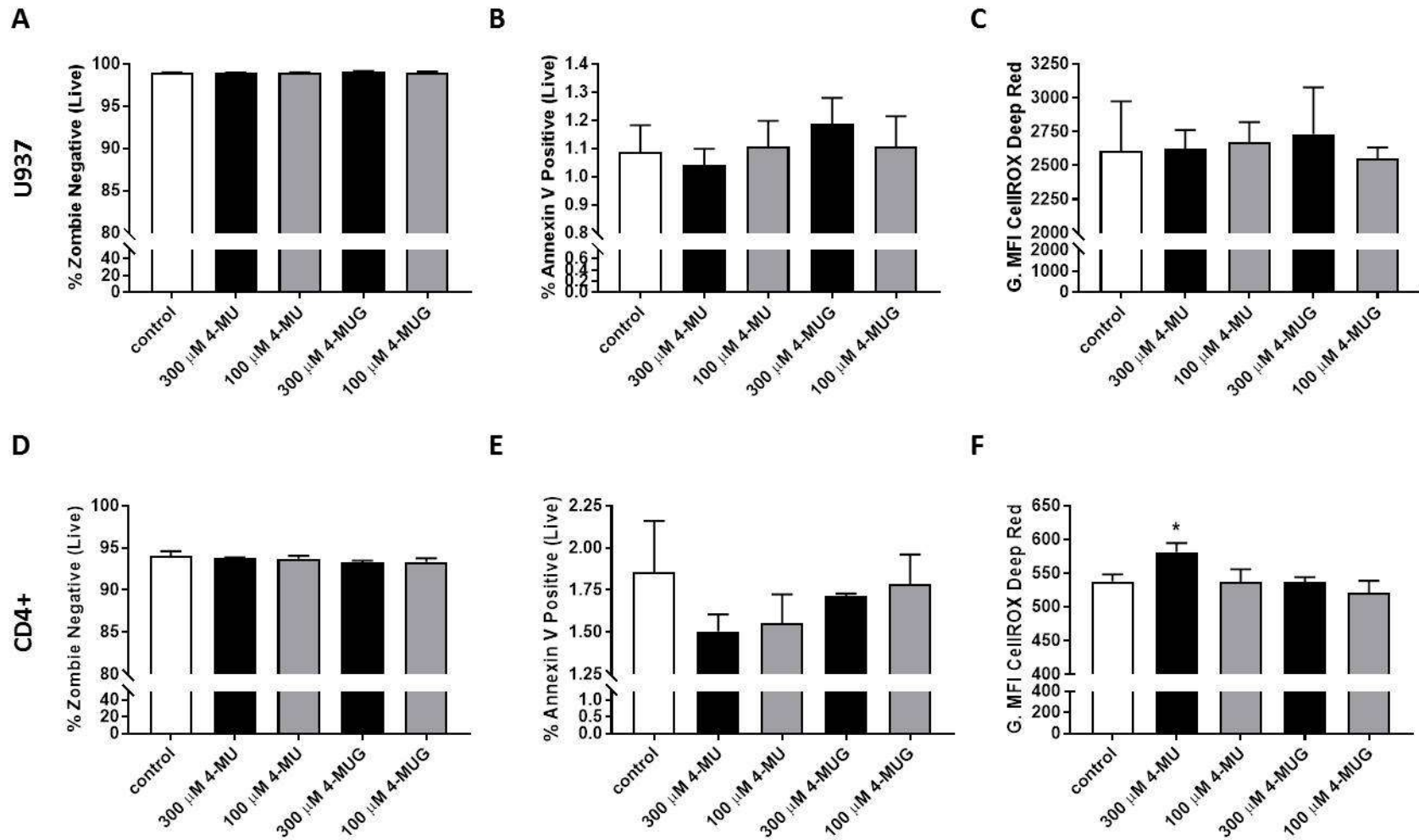
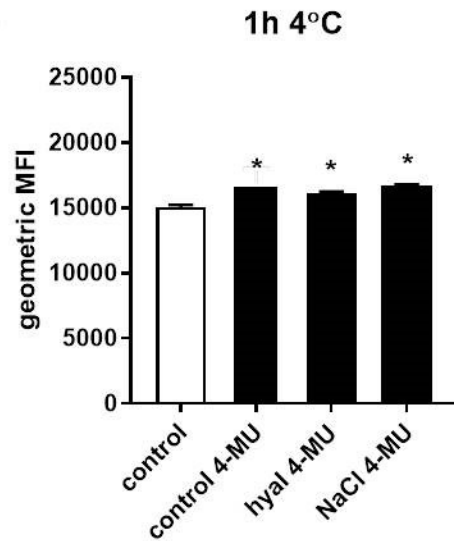
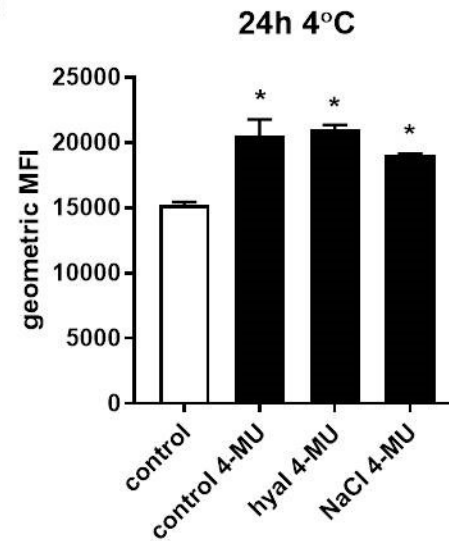
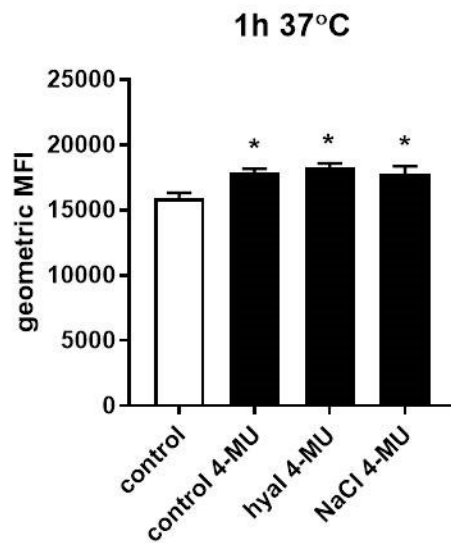
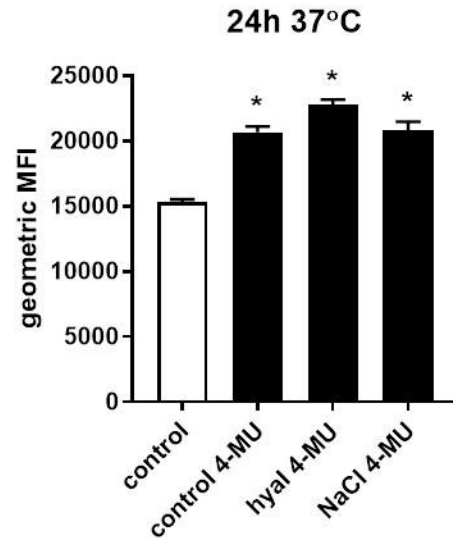


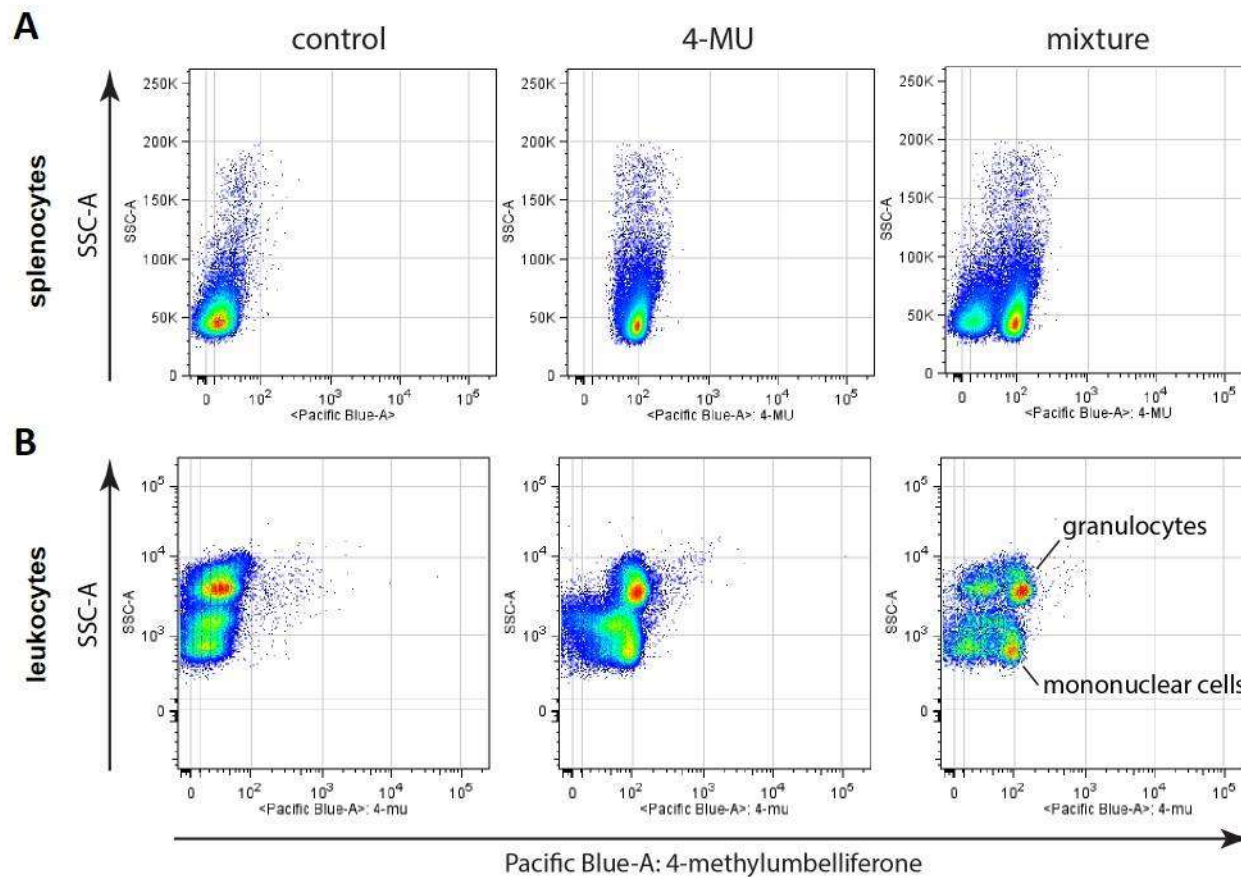
Supplemental Figure 1. 4-MUG does not inhibit GAG production. B16F10 cells were treated for 24 hours with 4-MU and 4-MUG at 300 μM and 100 μM concentrations. The cell pellet was used to measure the GAG concentration using the DMMB assay. N = 4 samples per condition.



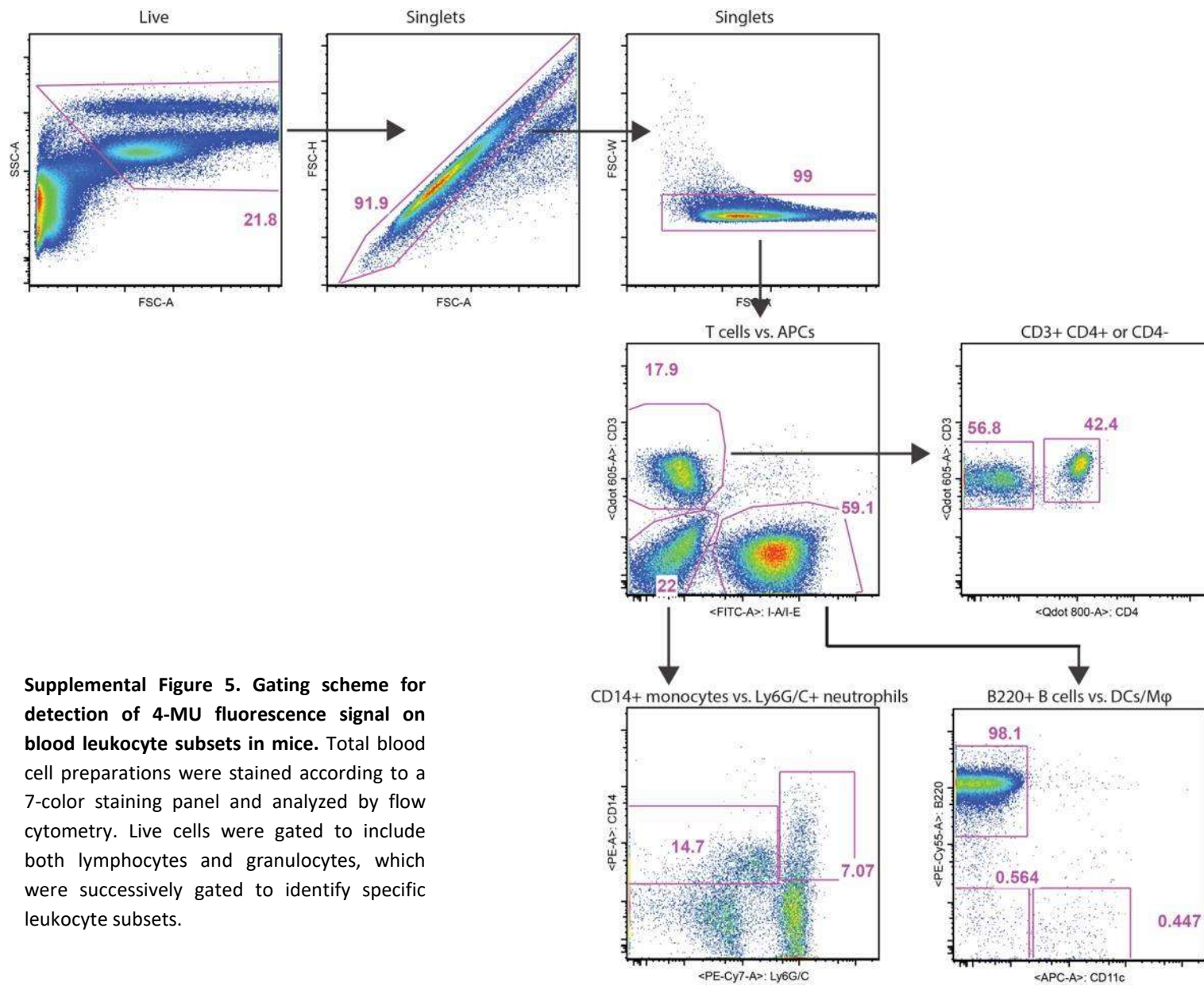
Supplemental Figure 2. 4-MUG does not produce measurable increases in ROS production or decreases in viability of mouse and human leukocytes. Human U937 cells (A-C) and activated mouse DO11.10 CD4+ T cells (D-F) were cultured for 24 hours in either 4-MU or 4-MUG at 300 μ M or 100 μ M concentrations. Percent viability (A,D) percent Annexin V positive (B,E), and ROS levels (C,F) were measured via flow cytometry. Data shown for n = 4 samples per condition. *p < 0.05 by One way ANOVA with Bonferroni post-test versus control.

A**B****C****D**

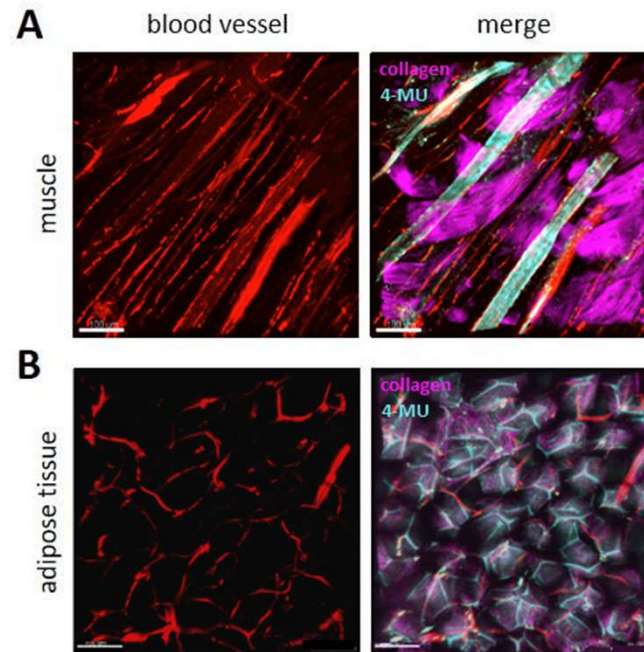
Supplemental Figure 3. 4-MU does not directly bind to HA. B16F10 cells were treated with 4-MU for 1 hour (A, C) or for 24 hours (B, D). Cells were kept at 4 degree Celsius (A, B) or 37 degree Celsius (C, D). After their 4-MU incubation time, cells were treated with hyaluronidase or washed three times with a NaCl salt wash. 4-MU signal was analyzed by flow cytometry, as measured in the Pacific Blue channel. Data shown for n = 4 samples per condition. *p < 0.05 by One way ANOVA with Bonferroni post-test versus control.



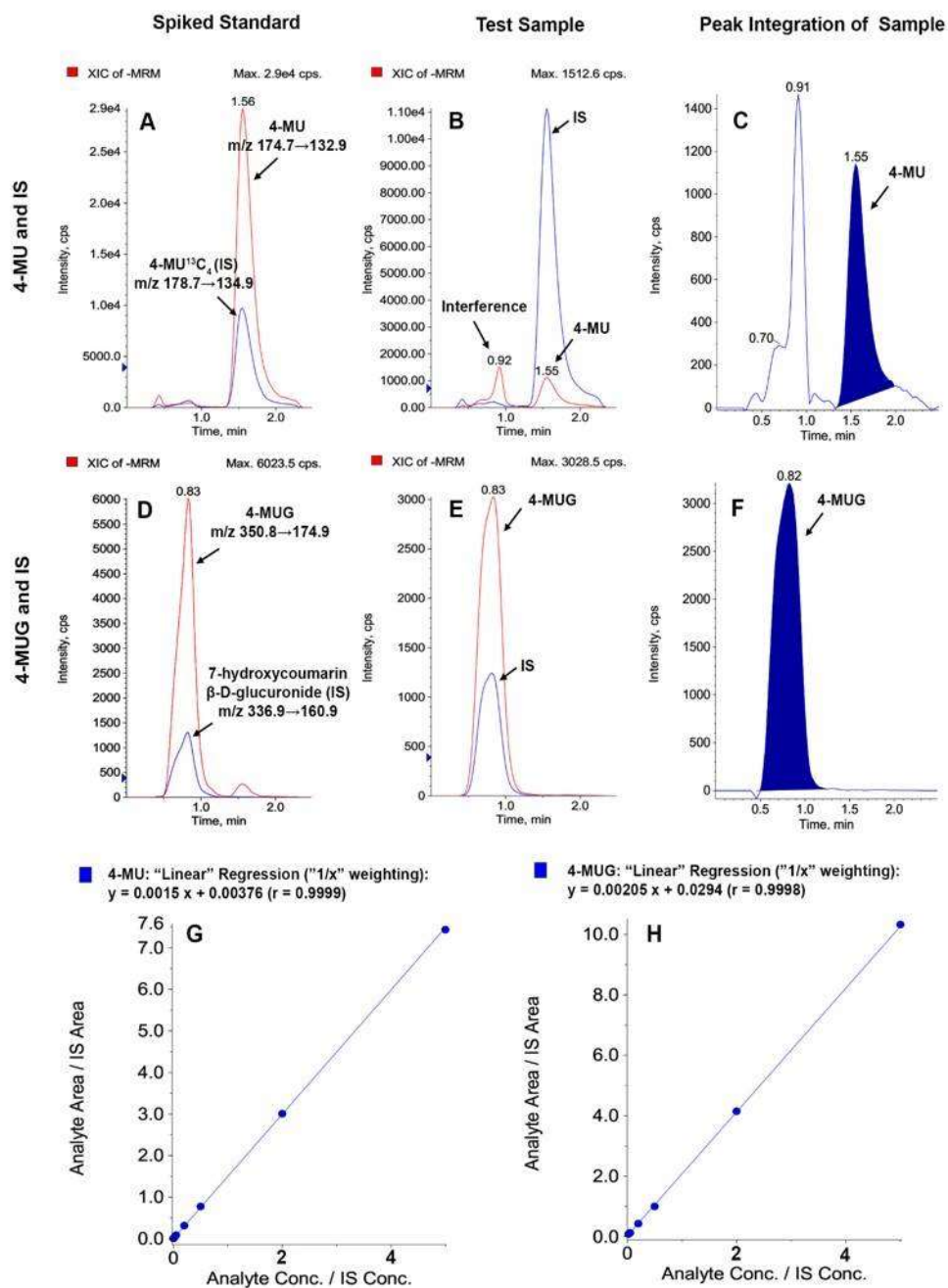
Supplemental Figure 4. 4-MU fluorescence is detectable on cells isolated from 4-MU treated mice. Mice were treated with 4-MU for at least 14 days, after which cells were isolated from spleen tissue (A) and blood (B). 4-MU signal was analyzed by flow cytometry, as measured in the Pacific Blue channel. Shown are representative single-cell populations from an untreated mouse (control), a 4-MU treated mouse (4-MU) or a combination (mixture) of cells from both mice.



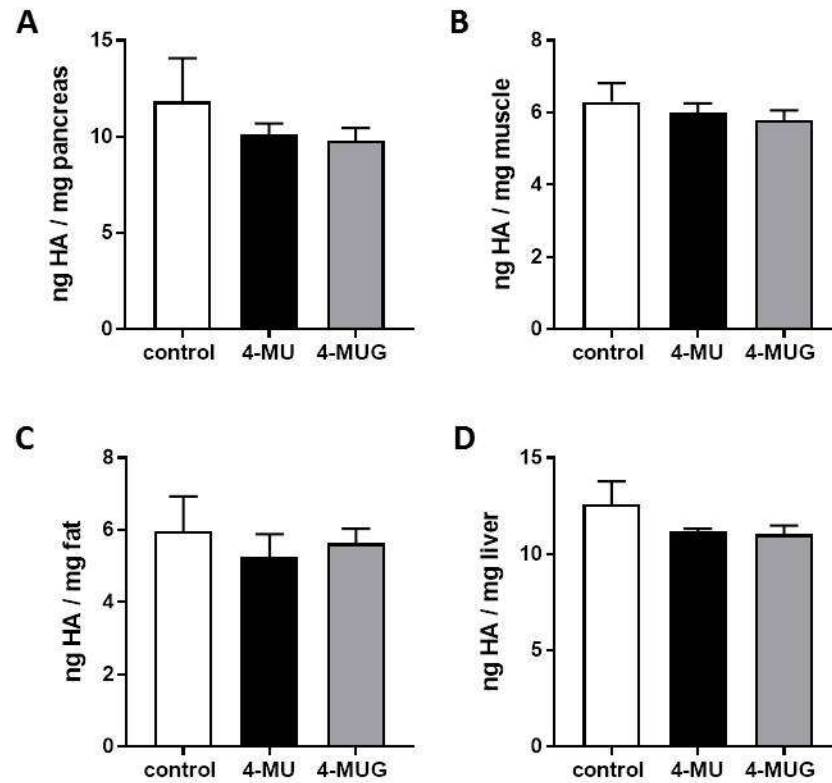
Supplemental Figure 5. Gating scheme for detection of 4-MU fluorescence signal on blood leukocyte subsets in mice. Total blood cell preparations were stained according to a 7-color staining panel and analyzed by flow cytometry. Live cells were gated to include both lymphocytes and granulocytes, which were successively gated to identify specific leukocyte subsets.



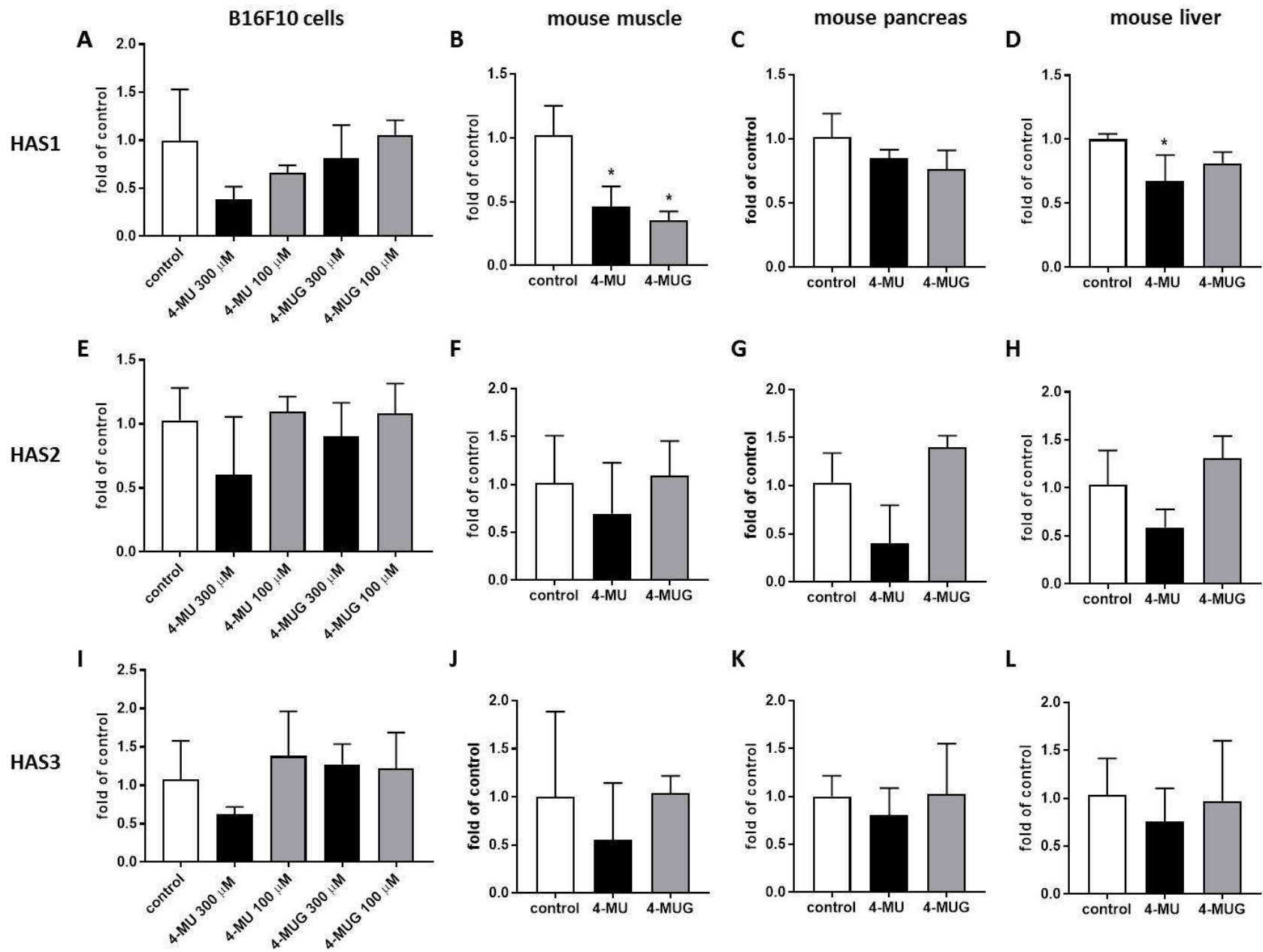
Supplemental Figure 6. Fluorescent 4-MU signal is independent of blood vessels. Tissue distribution of blood vessels is shown in mice treated with 4-MU (B) and 4-MUG (A). Representative images showing blood vessels, 4-MU and collagen signals in muscle (A) and adipose mouse tissue (B). The same muscle and adipose tissue images without blood vessels are shown in Figure 6B (muscle) and Figure 5C (adipose tissue). In each of those tissues blood vessels are shown in red, 4-MU has a specific distribution as shown at 810 nm wavelength. Collagen was visualized at 920 nm, the channels were merged for better structural orientation in the tissue. A-D, Scale bar = 100 μ m.



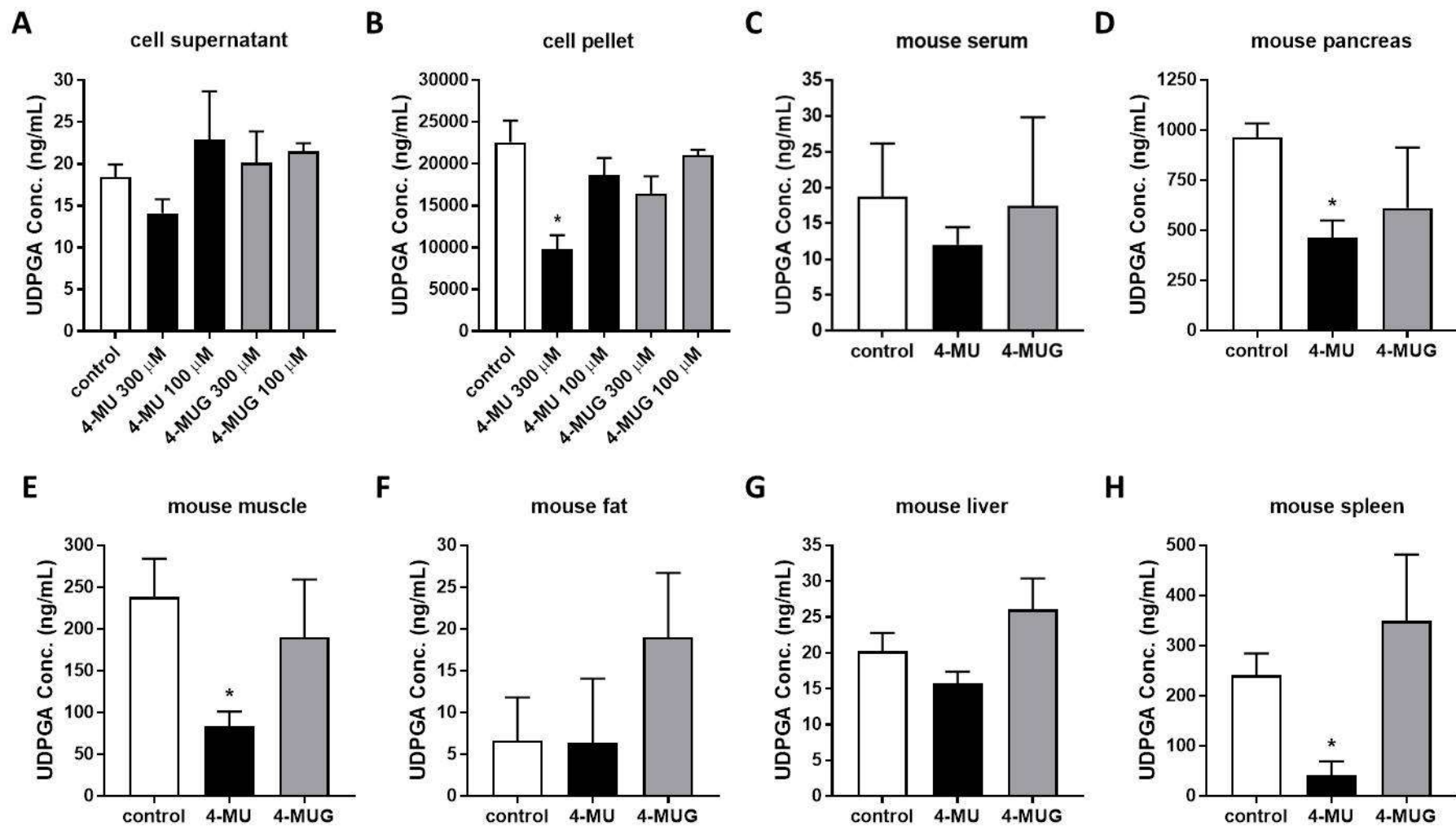
Supplemental Figure 7. LC-MS/MS analysis of 4-MU and 4-MUG. Representative chromatograms of a standard spiked with both 4-MU and 4-MUG (A and D) and a test sample (B and E) as well as the peak integration of the targeted analytes of the same test sample (C and F). A-C show the extracted ion current (XIC) of 4-MU (m/z 174.7→132.9) and/or 4-MU-13C₄ (m/z 178.7→134.9) as its internal standard. D-F show the XIC of 4-MUG (m/z 350.8→174.9) and/or 7-hydroxycoumarin β-D-glucuronide (m/z 336.9→160.9) as its internal standard. G and H show calibration curve of 4-MU and 4-MUG respectively.



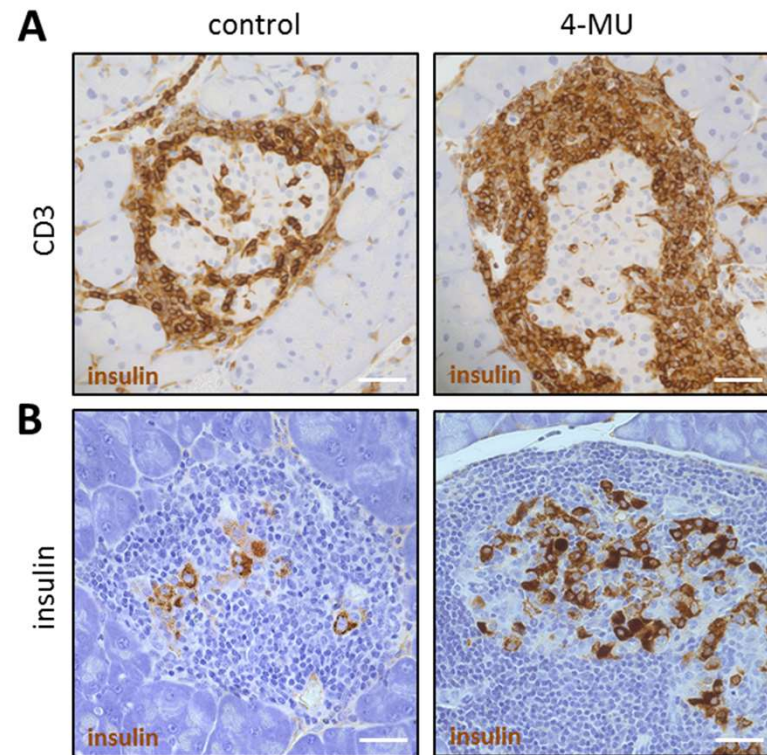
Supplemental Figure 8: 4-MU and 4-MUG treatment slightly reduces HA content in different mouse tissues. Mice were treated with 4-MU and 4-MUG for 2 weeks, tissues were harvested and HA content was measured in a HA ELISA. HA content in Pancreas (A), muscle (B), fat (C) and liver (D) are shown as ng HA per mg tissue. Data shown for n = 3 mice per treatment.



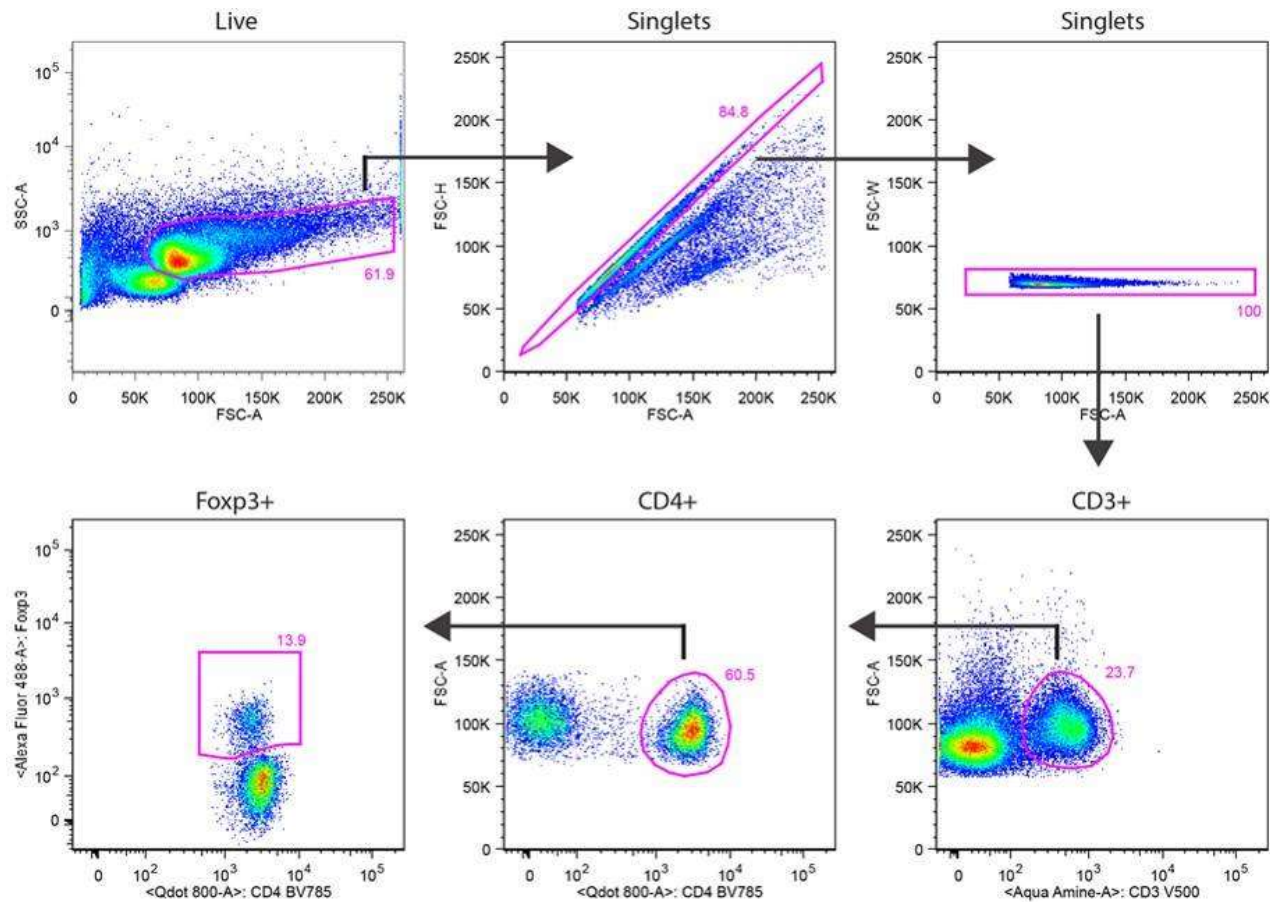
Supplemental Figure 9. 4-MU slightly alters HAS1-3 expression in cells and mouse tissues. B16F10 cells were treated for 24 hours with 4-MU and 4-MUG at 300 μ M and 100 μ M. Gene expression of HAS1 (A), HAS2 (E) and HAS3 (I) was determined by real time PCR. Mice were treated for 2 weeks with 4-MU and 4-MUG, organs were harvested and gene expression of HAS1-3 was measured by real time PCR. Gene expression of HAS1 was measured in muscle (B), pancreas (C) and liver (D). Gene expression of HAS2 was measured in muscle (F), pancreas (G) and liver (H). Gene expression of HAS3 was measured in muscle (J), pancreas (K) and liver (L). Data are shown for cell triplicates and n = 3 mice per treatment group. *p < 0.05 by One way ANOVA with Bonferroni post-test versus control.



Supplemental Figure 10. 4-MUG does not alter the UDPGA content in cells or mouse tissues. B16F10 cells were treated with 4-MU and 4-MUG for 24 hours (A, B). Mice were treated with 4-MU and 4-MUG for 2 weeks (C, H), tissues were harvested. The UDPGA content in the cell supernatant (A) as well as in the cell pellet (B) was measured. The UDPGA content in mouse serum (C), pancreas (D), muscle (E), fat (F), liver (G) and spleen (H) was measured using LC-MS/MS. Data are shown for n = 3 mice per treatment group. *p < 0.05 by One way ANOVA with Bonferroni post-test versus control.



Supplemental Figure 11. Insulinitis is accompanied with insulin loss in DORmO mice. Representative histologic staining of pancreatic tissue from untreated and treated DORmO mice. Pancreatic islets were stained for CD3 (A) and insulin (B), positive staining is shown in brown. Scale bar = 20 μ m.



Supplemental Figure 12. Gating scheme for the quantification of Foxp3+ regulatory T-cell numbers in mice. Splenocyte preparations were stained according to a 3-color staining panel and analyzed by flow cytometry. Live lymphocytes were successively gated to identify Foxp3+ regulatory T-cells amongst CD3+/CD4+ cells.